T. Zeev-Ben-Mordehai[1]
I. Silman[2]
J. L. Sussman[1]
[1]*Department of Structural Biology, Weizmann Institute of Science, Rehovot 76100, Israel*

[2]*Department of Neurobiology, Weizmann Institute of Science, Rehovot 76100, Israel*

Received 7 August 2002; accepted 15 August 2002

Acetylcholinesterase in Motion: Visualizing Conformational Changes in Crystal Structures by a Morphing Procedure

Abstract: *In order to visualize and appreciate conformational changes between homologous three-dimensional (3D) protein structures or protein/inhibitor complexes, we have developed a user-friendly morphing procedure. It enabled us to detect coordinated conformational changes not easily discernible by analytic methods or by comparison of static images. This procedure was applied to comparison of native* Torpedo californica *acetylcholinesterase and of complexes with reversible inhibitors and conjugates with covalent inhibitors. It was likewise shown to be valuable for the visualization of conformational differences between acetylcholinesterases from different species. The procedure involves generation, in Cartesian space, of 25 interpolated intermediate structures between the initial and final 3D structures, which then serve as the individual frames in a QuickTime movie.* © 2003 Wiley Periodicals, Inc. Biopolymers 68: 395–406, 2003

Keywords: *acetylcholinesterase; fasciculin; morphing; conformational change; organophosphate*

INTRODUCTION

Acetylcholinesterase (AChE) is responsible for the terminating impulse transmission at cholinergic synapses by rapid hydrolysis of the neurotransmitter acetylcholine (ACh).[1] Its key role makes it the target of nerve gases, pesticides, snake venom toxins, and anti-Alzheimer drugs.[1–6]

The three-dimensional (3D) structure of the enzyme from *Torpedo californica* (*Tc*AChE) was determined by x-ray crystallography in 1991.[7] The crystal structure reveals a single-domain protein, containing

Correspondence to: J. L. Sussman; email: Joel.Sussman@weizmann.ac.il

Contract grant sponsor: U.S. Army Medical and Material Command (USAMMC), the EC 5th Framework Program on the Quality of Life and Management of Living Resources, the Kimmelman Center for Biomolecular Structure and Assembly, and the Benoziyo Center for Neuroscience (Rehovot, Israel)

Contract grant number: DAMD17-97-2-7022

Biopolymers, Vol. 68, 395–406 (2003)

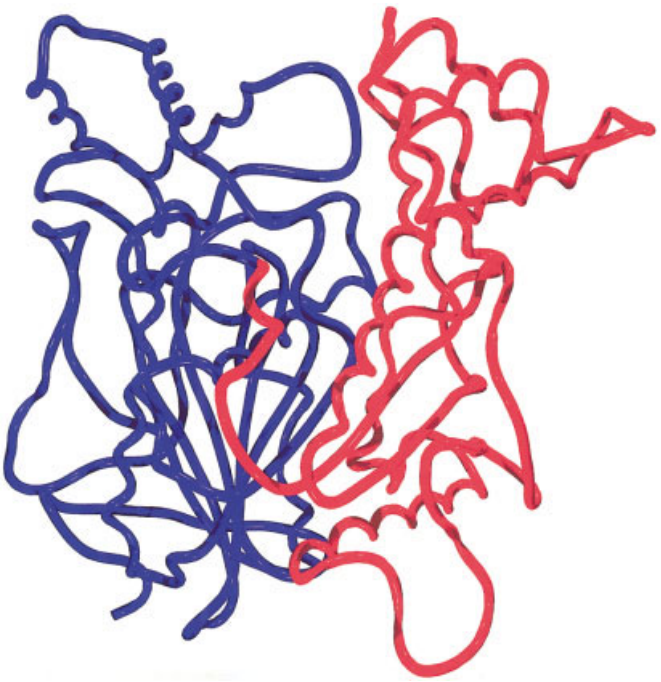

FIGURE 1 C_α trace of the 3D structure of *Tc*AChE. Residues 4–305 are colored blue, and residues 306–535 are colored red, highlighting the division of the molecule into two subdomains.

537 amino acids, with an overall α/β hydrolase fold.[8] *Tc*AChE is a serine hydrolase. Its active site lies near the bottom of a deep and narrow cavity, named the active-site gorge, which is about 15 Å deep. The structure can be further divided into two subdomains, each comprising one contiguous segment of the polypeptide: domain 1, residues 1–305, and domain 2, residues 306–537 (Figure 1). The active-site gorge is lined by residues derived from both subdomains.[9]

Since solution of the crystal structure of *Tc*AChE, those of AChEs from three other species have been solved: those of mouse AChE[10,11] (mAChE), human AChE[12] (hAChE), and *Drosophila* AChE[13] (*Dm*AChE). In addition, a repertoire of structures, primarily of *Tc*AChE, either complexed with reversible ligands, or conjugated with covalent inhibitors, have been reported (for literature, see Refs. 14 and 15). Currently ca. 30 such structures have been deposited in the Protein Databank (PDB). All four native structures have a similar overall fold, but *Dm*AChE, which shares only 36% sequence identity with the other three, differs substantially in some of its outer loops and in the dimensions and other features of the active-site gorge.[13] In general, the protein backbones of the complexes and conjugates do not differ substantially from their native counterparts; but as the number of structures solved has increased, such differences are becoming increasingly apparent, though often quite subtle.[16–18]

Morphing, a computer graphics technique that has been used for more than two decades, permits smooth transition from one structure or pattern to another. Tom Brigham used a form of morphing in experimental art at New York Institute of Technology in the early 1980s. Industrial Light and Magic used morphing for cinematic special effects in such movies as *Indiana Jones and the Last Crusade* as reviewed by Wolberg.[19] It is increasingly being applied to pattern recognition in general and for analyzing macromolecular motions in particular.[20] We have developed a *user-friendly*, straightforward procedure that permits us to readily morph from one protein structure to another, and thus to perceive subtle conformational differences and/or transitions that might not be detected or fully appreciated either by visual comparison of discrete structures or by computational procedures.

METHODS

Structural Alignment

Coordinates of structures employed were retrieved from the PDB. The native *Tc*AChE structure (PDB code 1ea5) was

taken as the reference structure. All others were structurally aligned to native *Tc*AChE using the LSQMAN package.[21] The alignment was accomplished in two steps: (1) explicit least-squares superposition; (2) improvement of the matrix relating the two structures by omitting the most divergent parts. This was done by employing a 3.5 Å distance cutoff and requiring a minimal fragment length of 5 contiguous residues. The rotation/translation operator obtained was applied to the second structure. This would be either the structure of a *Tc*AChE complex or conjugate with an inhibitor, or the structure of an AChE from another species.

Interpolation

The putative conformational transition from one structure to another was modeled by a series of interpolated intermediate model structures calculated by use of the morphing option in the LSQMAN package.[21] All transitions were morphed in Cartesian space since, in all cases examined, there are one or more large torsion-angle changes between the initial and final structures. It has been observed by Kleywegt[22] that "If one of the torsions changes a lot, this means that all residues C-terminal of it will swing with it, which may lead to very strange effects . . . ." When morphing in Cartesian space, every atom moves in a straight line from its initial to its final position. Morphing was implemented on each atom independently for the entire initial structure. For the cross-species transition, the input residue range was fragmented to ensure that the equivalent residues in the two sequences (structures) were matched correctly. For all morphing procedures, 25 interpolated intermediate structures were calculated. The output consisted of 25 PDB files containing the coordinates of the models, in which the *B* factor for each residue was replaced by the distance between the positions of its C_α in the initial and final models. The correctness of the intermediate models was validated visually using the O program.[23]

Animation

The PDB files were converted to RGB images, via the molecular graphics program RasMol,[24] with each image file serving as a single frame in the movie. Since this procedure results in freezing the image displayed, the coloring scheme, the style of display, and the orientation for visualization were all specified before writing the images into files. In order to compose the movie, all frames (images) were collated into one QuickTime format file by the MediaConvert program[25] on a Silicon Graphics (SGI) workstation. The resulting file is viewable via the QuickTime program[26] (with ".mov" extension) on virtually all computer platforms, e.g., PC, Mac, Unix.

RESULTS

In principle, conformational differences between native proteins and their conjugates with ligands, or between the same protein from different species, can be assessed by a variety of analytical procedures. In practice, however, the size of an individual protein structure, and the complex nature of its motifs and folds, often makes such conformational differences difficult to detect and assess. The morphing procedure utilized in the present study serves as a powerful method for visualizing significant, though often subtle, conformational changes, as will be apparent from the examples presented and discussed below.

Morphing from Native *Tc*AChE to Organophosphoryl Conjugates

Organophosphorus (OP) agents act as powerful inhibitors of AChE by interacting covalently with its active-site serine.[27,28] This is the basis for their toxicity and thus for their potency as nerve agents and insecticides.[2,29] Some OPs, subsequent to this covalent modification, undergo a reaction called "aging," which involves dealkylation of the bound OP moiety.[16,30] One such reagent is diisopropylfluorophosphate (DFP) that, subsequent to phosphorylation and "aging," yields the monoisopropylphosphoryl (MIP)/*Tc*AChE conjugate whose 3D structure was solved.[30] The crystal structure revealed that the bulky isopropyl group distorts the acyl-binding pocket, which normally recognizes the acetyl group of the substrate, ACh (Figure 2). The two structures have a root mean square deviation (RMSD) of 0.36 Å for 530 C_α atoms. The transition from native *Tc*AChE (PDB code 1ea5) to the MIP/*Tc*AChE conjugate (PDB code 2dfp) is morphed in a movie (http://www.weizmann.ac.il/~joel/moveis.html) of which three superimposed frames, the initial, the final, and one intermediate frame, are displayed in Figure 3.

The movie shows that phosphorylation by DFP causes a movement of the main chain in the conserved loop (residues 279–291), which includes the acyl pocket residues, F288 and F290, as reported by Millard and co-workers.[30] However, this major movement of residues in the acyl pocket also affects part of the peripheral site, which is on the same loop (viz. W279); this, in turn, causes substantial movement of residues in the second subdomain, across the active-site gorge, with which the 279–291 loop is in contact.[9] This is also shown by color coding the *movements* between native *Tc*AChE and the MIP conjugate on a scale from blue to red, going from the smallest to the largest differences (Figure 3).

For comparison, we show the transition from native *Tc*AChE (PDB code 1ea5) to the *Tc*AChE/soman conjugate, viz. the methylphosphonyl con-

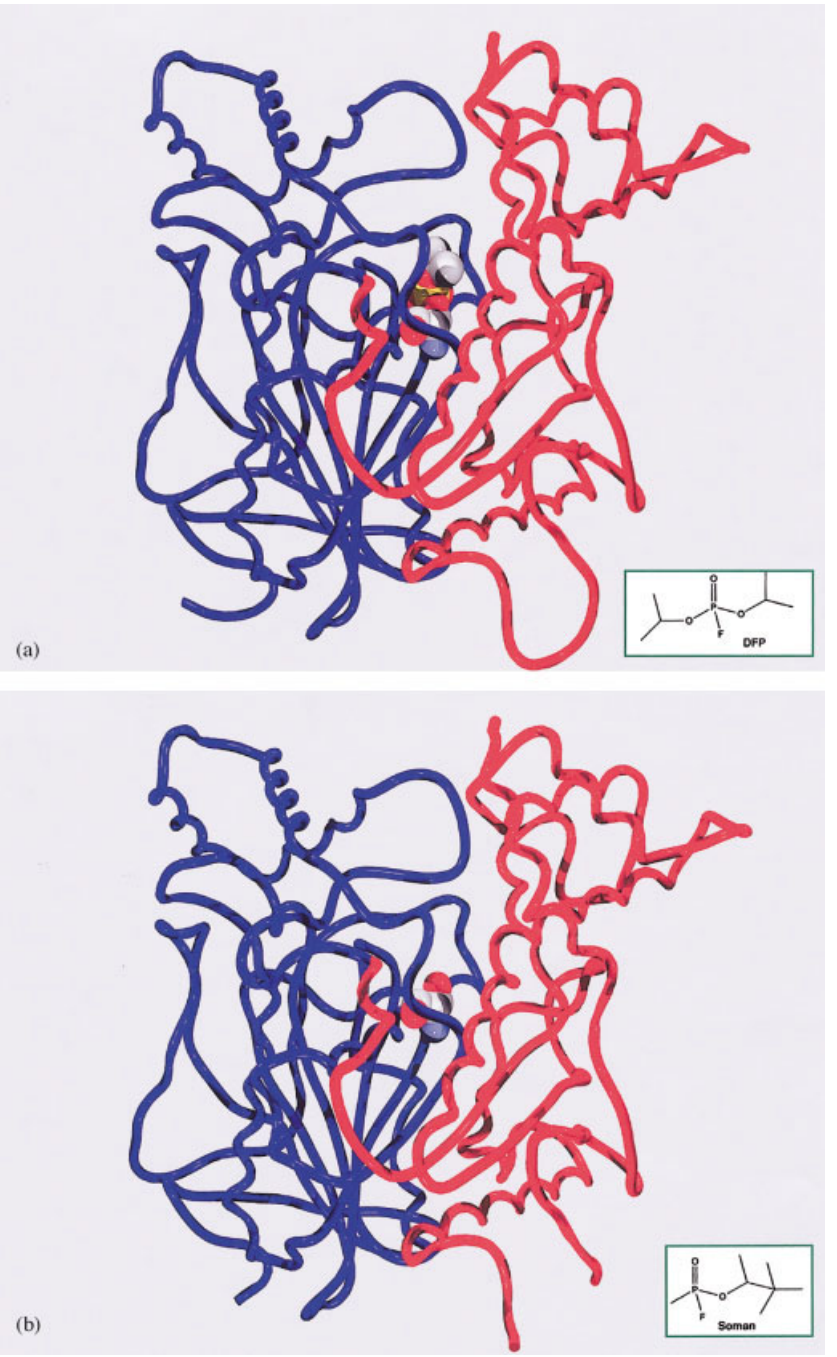

FIGURE 2 C_α traces of "aged" OP/*Tc*AChE conjugates. (a) MIP/*Tc*AChE, i.e., *Tc*AChE inhibited by DFP. Inset, chemical formula of DFP. (b) Methylphosphonyl/*Tc*AChE, i.e., *Tc*AChE inhibited by soman. Residues 486–489 were not seen in the electron density map of *Tc*AChE/soman,[30] and thus there is a break in the polypeptide chain near the bottom right portion of the structure, as has been observed for a number of AChE structures.[7] Inset, chemical formula of soman. Color coding of *Tc*AChE as in Figure 1. OP moieties shown as space-filling models.

jugate (PDB code 1SOM), for which the crystallographic data did not reveal any significant conformational change, with an RMSD of 0.16 Å for 528 C_α atoms. The corresponding movie (http://www.weizmann.ac.il/~joel/movies.html) indeed shows little or no movement, and the corresponding color-coded pictures show an almost uniformly blue C_α trace (Figure 4).

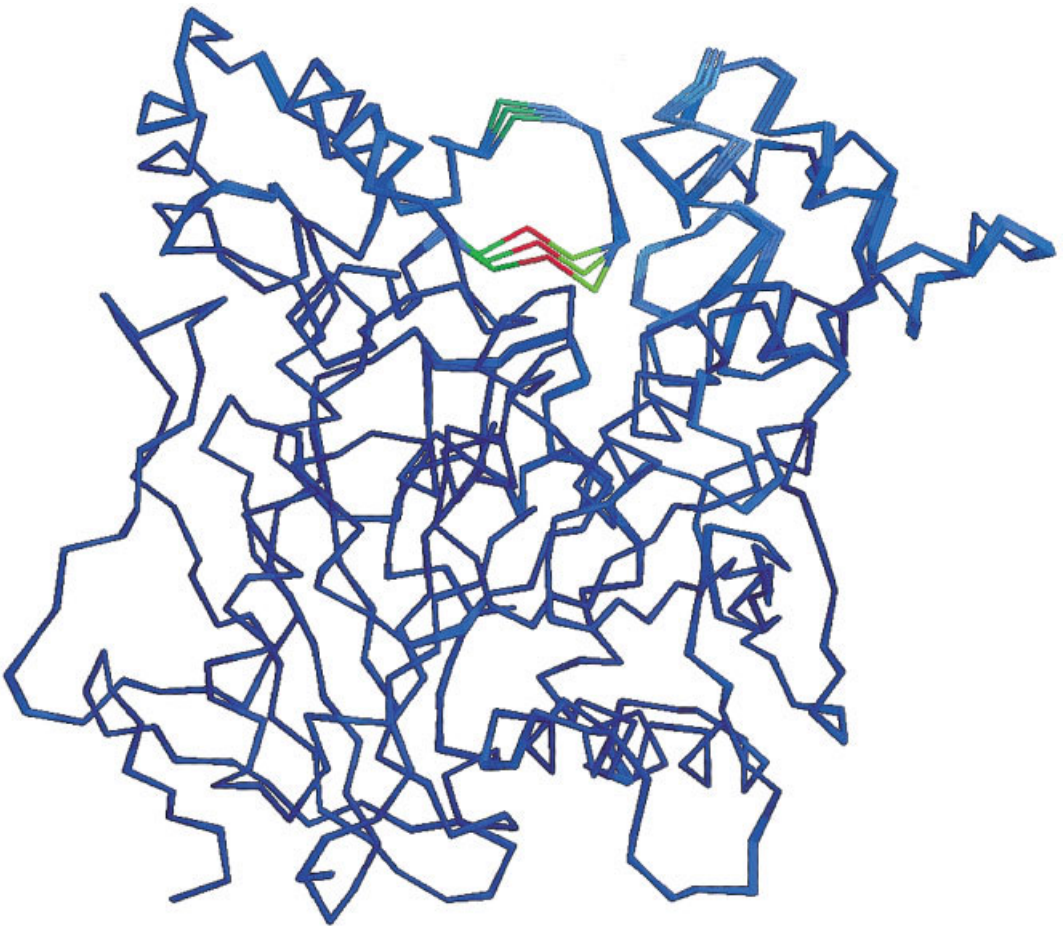

FIGURE 3 Morphing of the native *Tc*AChE structure to the MIP/*Tc*AChE structure. Superposition of three frames from the movie (http://www.weizmann.ac.il/~joel/movies.html), i.e., initial, middle, and final. Movement is coded on a blue-to-red scale, representing the distance for each C_α atom between its position in the initial and final model in ångstroms, with red corresponding to the largest displacements and blue to the smallest. This coloring scheme highlights movement of the main chain in the conserved loop (residues 279–291) and in the second subdomain.

Morphing from Native *Tc*AChE to Its Complex with Fasciculin-II

Fasciculin-II (FAS-II) is a member of the "three-fingered" polypeptide toxin family,[31,32] found in the venom of the green mamba, which inhibits vertebrate AChEs by binding tightly to the entrance of the active-site gorge.[32] Its inhibitory action is ascribed primarily to steric hindrance[10,12,33–36] but an allosteric component has also been invoked.[10,34,37–41] We thought it worthwhile, therefore, to utilize the morphing technique to visualize putative conformational changes occurring in the enzyme upon binding of the toxin.

Figure 5a shows the *Tc*AChE/FAS-II complex with the polypeptide positioned over the entrance to the active-site gorge; in Figure 5b this same structure is shown rotated 90° about the x axis. The movie (http://www.weizmann.ac.il/~joel/movies.html), in the same orientation as Figure 5b, shows the transition from native *Tc*AChE (PDB code 1ea5) to the *Tc*AChE/FAS-II complex (PDB code 1fss), with the FAS-II omitted to facilitate visualization of the changes in the *Tc*AChE polypeptide. The RMS distance between the AChE chain of the two structures is 0.52 Å for 532 C_α atoms. The movie shows that the binding of FAS-II causes a local shift of residues, in comparison to native *Tc*AChE, as reported by Harel et al.[33] One can note a shift downward of the 279–291 loop in the first subdomain, on the left-hand side of the picture, and a concomitant upward shift of a loop containing Y334 and G335 in the second subdomain on the other side of the gorge. These movements are

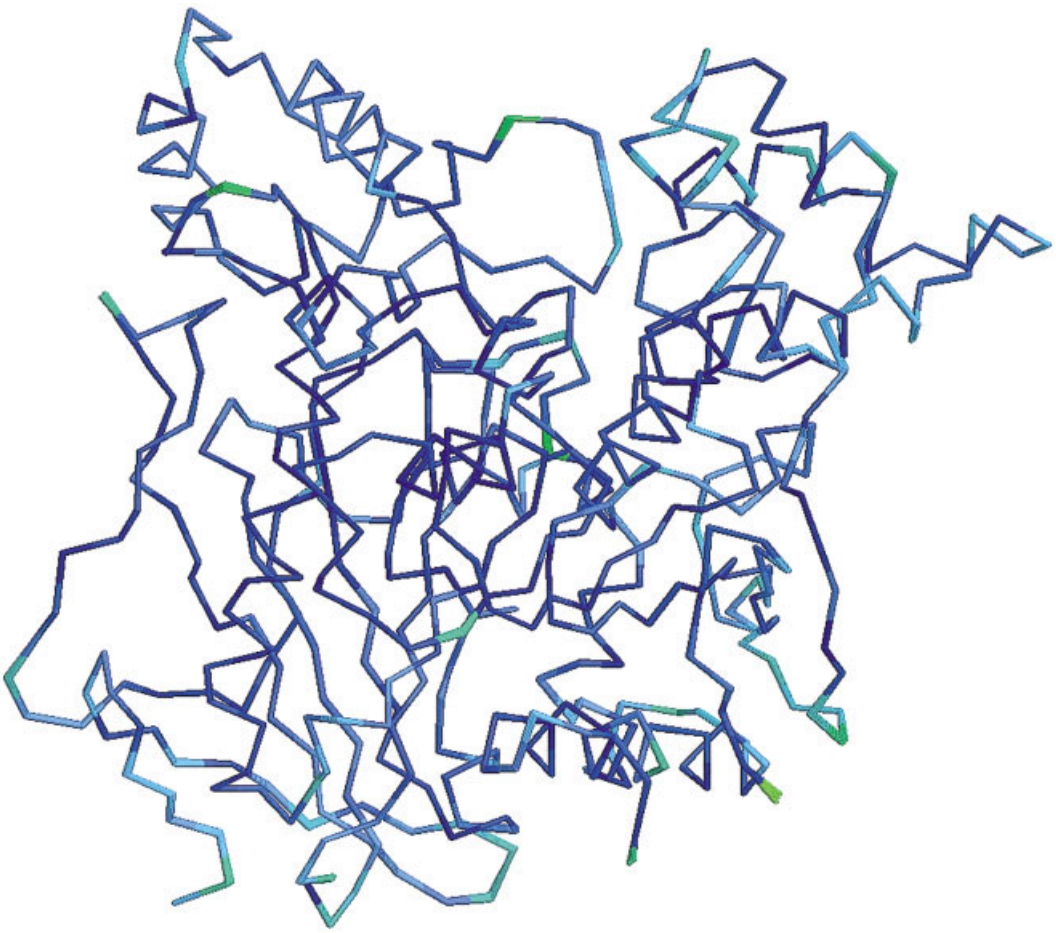

FIGURE 4 Morphing of the native *Tc*AChE structure to the methylphosphonyl/*Tc*AChE structure. Superposition of three frames from the movie (http://www.weizmann.ac.il/~joel/movies.html), i.e., initial, middle, and final. The almost uniformly blue C_α trace indicates little or no difference between the two structures. Color coding as in Figure 3. Residues 486–489 were not seen in this structure (see Figure 2b).

presumably driven by insertion of loop 2 of FAS-II into the mouth of the gorge. Inspection of Table 3 in Harel et al.[33] shows that both these loops, indeed, interact with FAS-II. In Figure 5b, the contact residues of FAS-II loop 2 are color coded in cyan and the contact residues on the complementary loops in the gorge of AChE are color coded in yellow. One can see the good correspondence of these color coded loops and the color code for movement in Figure 6 and in the corresponding movie. It is worth noting that in Figure 6 one can see also substantial movement of the omega loop in agreement with previous suggestions.[10,34,38–40] The color coding also suggests a slight movement of Ser200. It was earlier suggested on the basis of kinetic data that FAS-II acts predominantly by altering the conformation of the active site in the ternary complex, so that the steps involving proton transfer during enzyme acetylation are slowed.[37] Molecular dynamics simulation also suggested a disruption of the catalytic triad in the AChE/FAS-II complex.[41] A subtle movement of the triad residues would obviously suffice to affect catalytic activity profoundly.

Morphing from the *Tc*AChE/FAS-II Complex to the hAChE/FAS-II Complex

hAChE displays 53% sequence identity to *Tc*AChE, suggesting that their 3D structures should be very similar. This was indeed born out when the 3D structure of hAChE, complexed with FAS-II, was solved.[12] The RMSD between the *Tc*AChE/FAS-II complex (1fss, PDB code) and the hAChE/FAS-II complex (1b41, PDB code) is 0.88 Å for 521 C_α atoms[12] However, comparison of the two structures revealed a significant difference which involves flipping of the

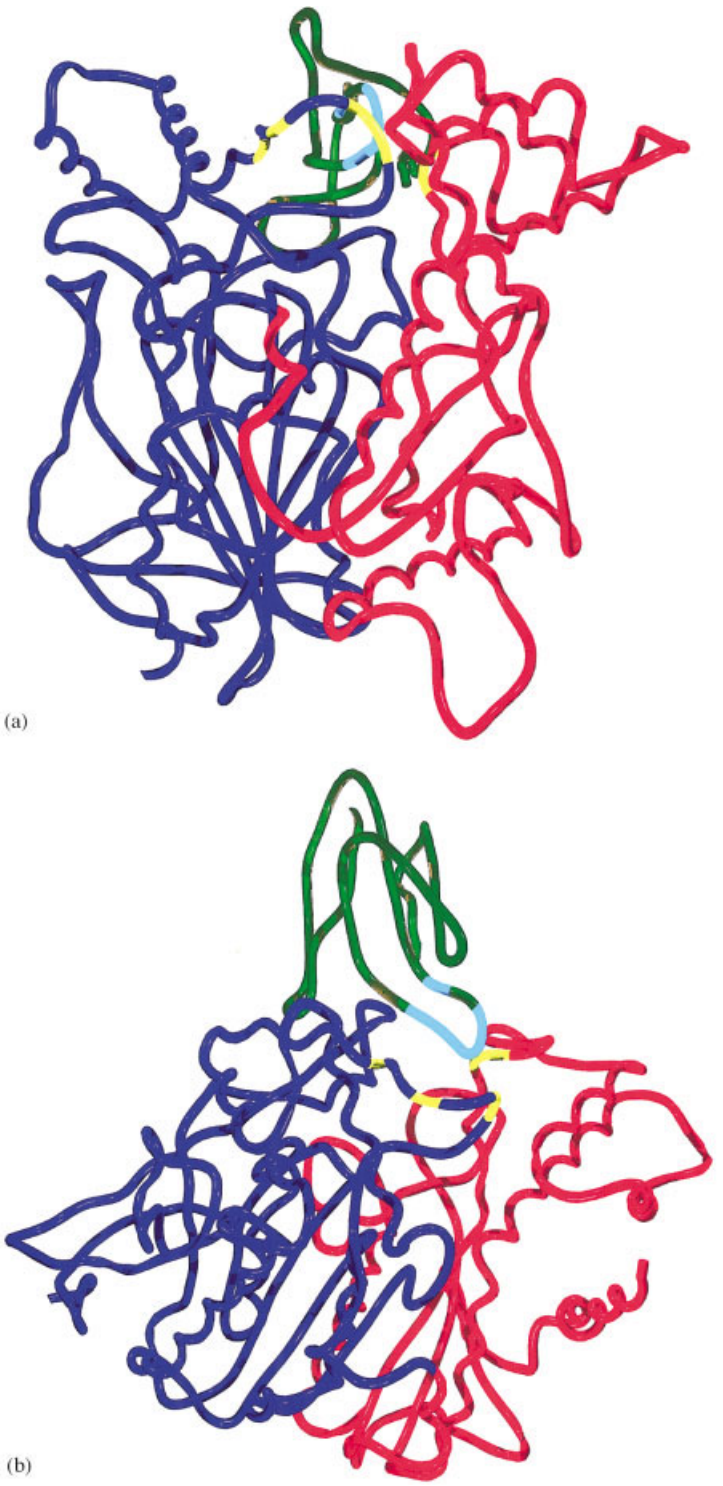

FIGURE 5 C_α trace of the 3D structure of the *Tc*AChE/FAS-II complex. (a) Entrance to active-site gorge at the top; (b) rotation ~90° about the *x* axis relative to (a). The *Tc*AChE subdomains are represented as in Figure 1, and FAS-II is color coded in green. Interacting residues of FAS-II loop 2 are colored cyan and the complementary interacting residues in *Tc*AChE are colored yellow.

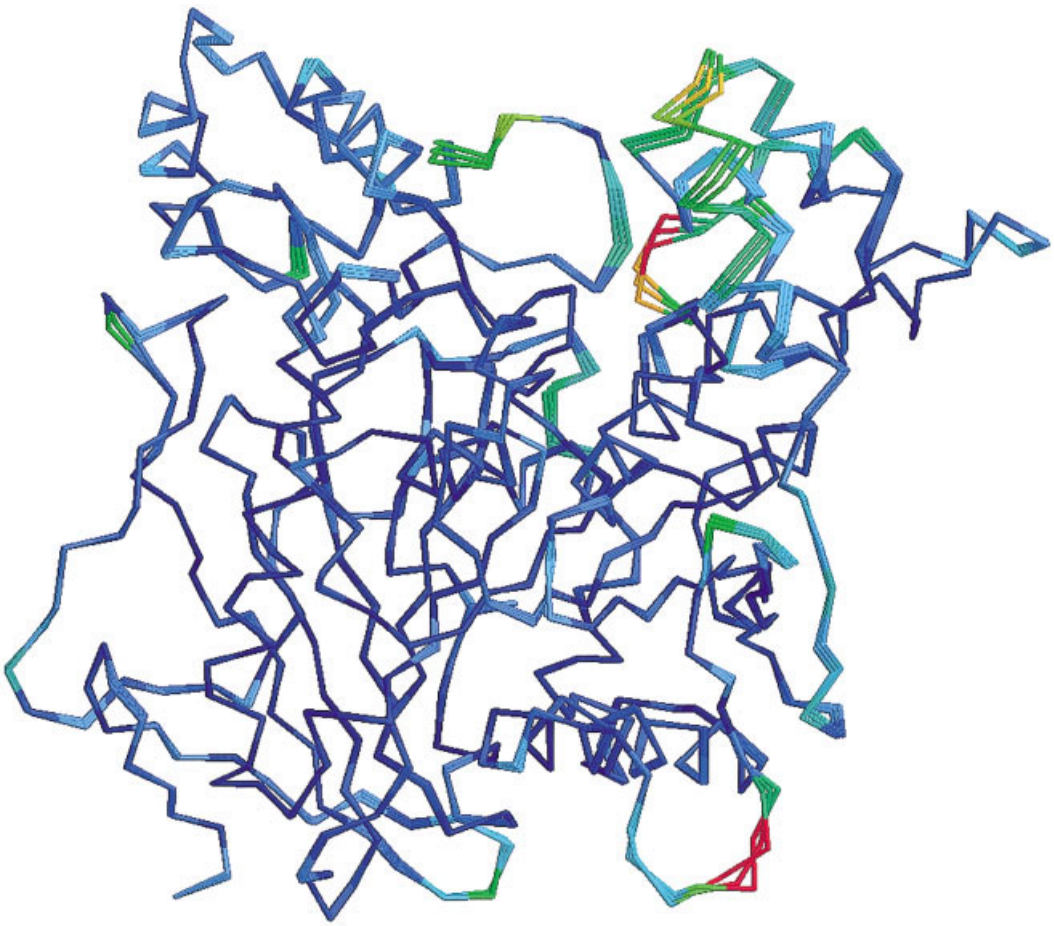

FIGURE 6 Morphing of the native *Tc*AChE structure to the *Tc*AChE/FAS-II complex. Superposition of three frames from the movie (http://www.weizmann.ac.il/~joel/movies.html), i.e., initial, middle, and final. One sees good correspondence of the color coding, indicating substantial movement of the conserved 279–291 loop, and of the loop containing Y334 and G335, across the active-site gorge, in the second subdomain, with the residues coded yellow in Figure 5. The apparent change in conformation of residues 486–489 is most likely a consequence of the known flexibility of this external loop, which often, indeed, is not seen in the electron density map (see Figure 2b).

310–317 loop (*Tc*AChE numbering).[12] This was not due to crystal contacts, as was established by comparison with the native mAChE structure,[11] and with that of the mouse AChE/FAS-II complex[10], both of which showed the same flip relative to the *Tc*AChE/FAS-II structure. In the movie (http://www.weizmann.ac.il/~joel/movies.html) of the transition from *Tc*AChE/FAS-II to hAChE/FAS-II, this flip is clearly visualized. However, the movie also highlights a correlated movement of an adjacent but noncontiguous loop, residues 413–417 (*Tc*AChE numbering), not reported previously (Figure 7).

Morphing from *Tc*AChE to *Dm*AChE

*Dm*AChE displays 36% sequence identity to *Tc*AChE. This homology is substantially lower than that between *Tc*AChE and hAChE; a similar fold was, nevertheless, to be expected, as was born out by the 3D structure of *Dm*AChE,[13] even though the similarity of the structures was not high enough to permit solution of the structure by molecular replacement based on the *Tc*AChE structure. The RMSD between the C_α atoms of *Tc*AChE (1ea5, PDB code) and *Dm*AChE (1qo9, PDB code), using 481 residues, is 1.28 Å. Although the geometry of the catalytic apparatus of the two enzymes is almost isomorphous, substantial differences were observed in the volume and geometry of the active-site gorge, as well as large differences in some of the distal loops.[13] In the movie (http://www.weizmann.ac.il/~joel/movies.html) of the transition from *Tc*AChE to *Dm*AChE one clearly sees, not surprisingly, much larger overall movements than in the previous movies. It is interesting, however,

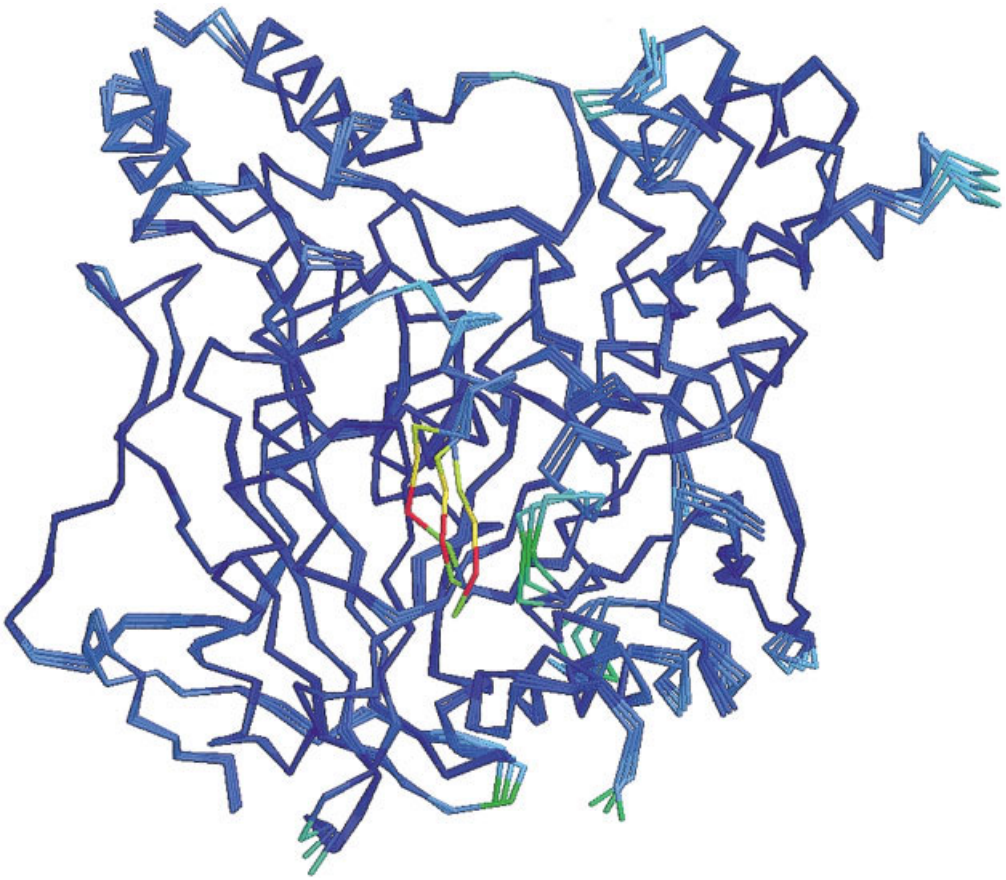

FIGURE 7 Morphing of the *Tc*AChE/FAS-II complex to the hAChE/FAS-II complex. Superposition of three frames from the movie (http://www.weizmann.ac.il/~joel/movies.html), i.e., initial, middle and final. In these pictures a correlated movement is seen of loops 413–417 and 310–317 (*Tc*AChE numbering). Color coding as in Figure 3. The absence of residues 486–489 in this movie is due to the fact that they are absent in the hAChE/FAS-II complex, as in a number of other AChE structures (see Figure 2b). Although they are present in the starting structure—viz., the *Tc*AChE/FAS-II complex—the absence of corresponding residues in the final model did not allow the automatic morphing procedure to process these residues.

that a flip of the two loops which flip in the transition from *Tc*AChE to hAChE is also observed in the *Tc*AChE/*Dm*AChE transition. The movie also shows a large movement in the region 333–337 relative to the 279–291 loop (*Tc*AChE numbering) on the opposite side of the top of the gorge. Since this region contains one of the helices (365–375) making up the four-helix bundle of the biological dimer, movement of this region, like a smaller one observed for hAChE relative to *Tc*AChE, is due to differences in the amino acid sequence in this region, and not to different crystallographic contacts in the *Tc*AChE vs the *Dm*AChE crystal structures. This movie shows, in addition, coordinated movement of a third loop, residues 216–221 (*Tc*AChE numbering), adjacent to the two loops just mentioned (Figure 8). Another difference between the *Tc*AChE and *Dm*AChE structures is at the entrance to the active-site gorge, and is highlighted using the morphing technique. There are two amino acids deleted in the conserved loop, 279–291 (*Tc*AChE numbering), i.e., residues 283–284 at the top of the gorge. This makes the *Dm*AChE loop smaller, which, in turn, increases the distance between the two subdomains (Figure 8).

DISCUSSION

Although a wide variety of tools are available for analysis of structural differences between related proteins, or between proteins and their complexes and conjugates with reversible or covalent ligands,[21,42-44] the ability to visualize the morphing between pairs of

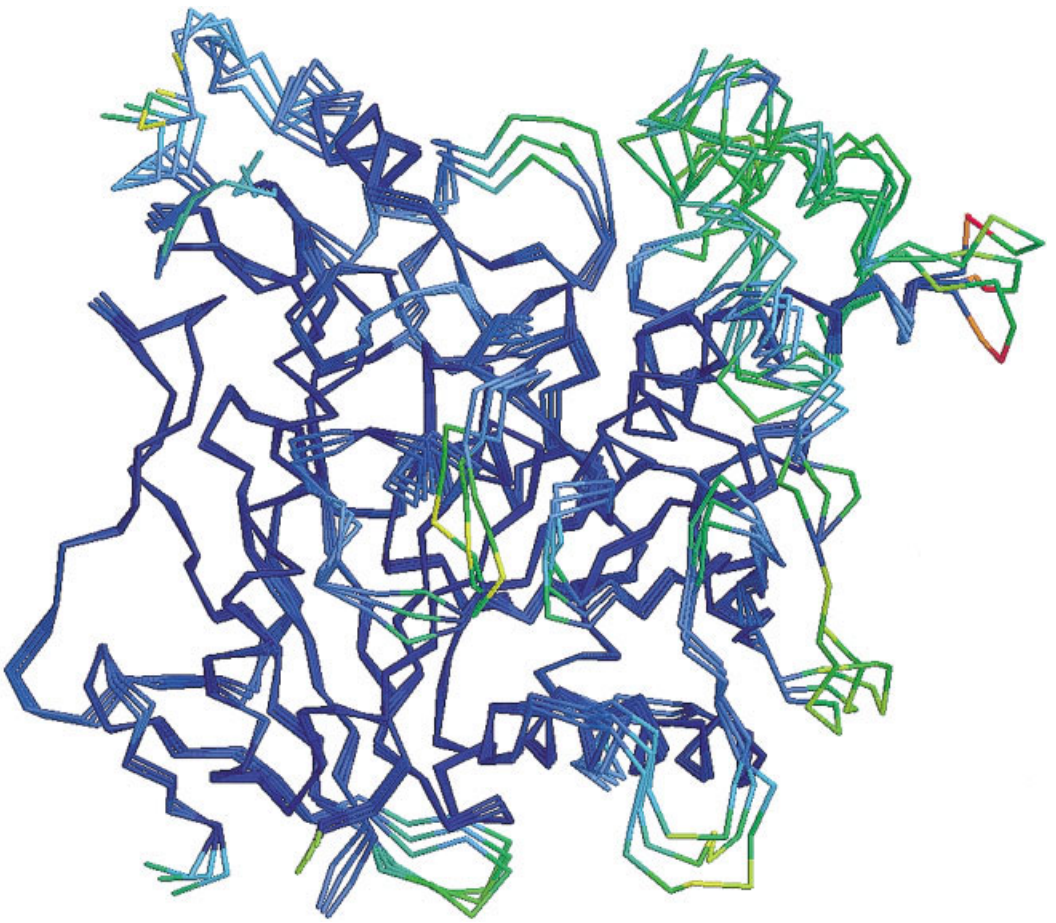

FIGURE 8 Morphing of the native *Tc*AChE structure to the native *Dm*AChE structure. Superposition of three frames from the movie (http://www.weizmann.ac.il/~joel/movies.html), i.e., initial, middle, and final. These pictures clearly show a similar flipping of loops as observed in the transition from *Tc*AChE to hAChE (residues 310–317, 413–417; *Tc*AChE numbering). In addition, a large movement is observed in subdomain 2 across from the conserved loop 279–291 in subdomain 1.

structures often reveals differences not otherwise readily perceived.

One of the most illustrative examples of the use of morphing was in the case of the four different crystal structures of adenyl kinase and of the movie produced to show the "motions" between these different forms[45] (see also: http://bio.chemie.uni-freiburg.de/ak_movie/). More recent progress in this area has been reviewed by Krebs and Gerstein[20] (see also http://bioinfo.mbb.yale).

In this study, we have developed a "user-friendly" tool to automate transitions between any pair of closely related protein structures. As described under Methods, our procedure utilizes Cartesian coordinates, and is not intended to faithfully reflect the "chemical" trajectory of a conformational change. However, it does make it possible to readily perceive and evaluate coordinated changes in structure that may occur when a ligand/protein complex is formed, or to evaluate conformational differences between closely related proteins from different species.

For example, our morphing technique clearly reveals the coordinated movements occurring in the two subdomains across the active-site gorge from each other upon distortion of the acyl pocket by covalent modification with DFP, or upon insertion of loop 2 of FAS-II into the mouth of the gorge. It also shows that these changes do not occur in all cases of ligand binding, e.g., for the *Tc*AChE/soman conjugate. The technique also highlights interspecies differences. Thus, comparison of the *Tc*AChE structure with those of both hAChE and *Dm*AChE shows a coordinated change in structure of several loops that would not be easily perceived from inspection of static structures.

The morphing movies can also reveal the nature of the conformational changes between structures—e.g.,

the apparent "spiral" movement of the two helices contributing to the four-helix bundle of the dimer in both *Tc*AChE and *Dm*AChE (viz. helices $\alpha_{F'3}$ and α_H in *Tc*AChE[7]).

When examining the apparent conformational changes between any pair of structures, care must be exercised to ascertain that the apparent differences are not a trivial consequence of different crystallographic packing. For the native vs *Tc*AChE conjugates, since the same crystal form was employed, this was not a problem. However, for native *Tc*AChE vs the *Tc*AChE/FAS-II complex, as well as for the cross-species comparisons, it was indeed a potential problem. For the case of the FAS-II complex, the FAS-II binds at virtually the same site as another *Tc*AChE binds in the native enzyme; thus in both cases the top of the gorge is making contacts, in fact, with another molecule, albeit in one case with another copy of *Tc*AChE and in the other case with a FAS-II molecule. For both the hAChE and *Dm*AChE structures, the major movements seen relative to the *Tc*AChE structure are found in the region of the two helices that form the four-helix bundle of the biological dimer. As this four-helix bundle is very similar in all three structures—i.e., *Tc*AChE, hAChE, *Dm*AChE—the large changes in structures seen in the morphing movies likely reflect real differences in conformation between these structures, reflecting the differences in amino acid sequences of the residues in the four-helix bundle and in adjacent parts of the structures.

The method we have developed is a "user-friendly" approach based on tying together a series of preexisting tools, and taking advantage of the capacity of the human visual system for subtle pattern recognition. What we have done here, using morphing techniques, is in the spirit of a study carried out in collaboration with Shneior Lifson in the cross-species analysis of electrostatic properties of AChE.[46] We feel that Shneior would have been delighted to see our current movies, and probably would have been able to perceive more than our eyes did.

This work was supported by the U.S. Army Medical and Material Command under Contract No. DAMD17-97-2-7022, the EC 5th Framework Program on the Quality of Life and Management of Living Resources, the Kimmelman Center for Biomolecular Structure and Assembly and the Benoziyo Center for Neuroscience (Rehovot, Israel). IS is the Bernstein-Mason Professor of Neurochemistry.

REFERENCES

1. Taylor, P. The Pharmacological Basis of Therapeutics, 9th Ed.; Hardman, J. G., Limbird, L. E., Molinoff, P. B., Ruddon, R. W., Gilman, A. G., Eds.; McGraw-Hill: New York, 1996; pp 161–176.
2. Millard, C. B.; Broomfield, C. A. J Neurochem 1995, 64, 1909–1918.
3. Davis, K. L.; Powchik, P. Lancet 1995, 345, 625–630.
4. Nightingale, S. L. JAMA 1997, 277, 10.
5. Casida, J. E.; Quistad, G. B. Ann Rev Entomol 1998, 43, 1–16.
6. Martin, R. J. Vet J 1997, 154, 11–34.
7. Sussman, J. L.; Harel, M.; Frolow, F.; Oefner, C.; Goldman, A.; Toker, L.; Silman, I. Science 1991, 253, 872–879.
8. Ollis, D. L.; Cheah, E.; Cygler, M.; Dijkstra, B.; Frolow, F.; Franken, S. M.; Harel, M.; Remington, S. J.; Silman, I.; Schrag, J.; Sussman, J. L.; Verschueren, K. H. G.; Goldman, A. Protein Eng 1992, 5, 197–211.
9. Morel, N.; Bon, S.; Greenblatt, H.; Wodak, S.; Sussman, J. L.; Massoulié, J.; Silman, I. Mol Pharmacol 1999, 55, 982–992.
10. Bourne, Y.; Taylor, P.; Marchot, P. Cell 1995, 83, 503–512.
11. Bourne, Y.; Taylor, P.; Bougis, P. E.; Marchot, P. J Biol Chem 1999, 274, 2963–2970.
12. Kryger, G.; Harel, M.; Giles, K.; Toker, L.; Velan, B.; Lazar, A.; Kronman, C.; Barak, D.; Ariel, N.; Shafferman, A.; Silman, I.; Sussman, J. L. Acta Cryst 2000, D56, 1385–1394.
13. Harel, M.; Kryger, G.; Rosenberry, T. L.; Mallender, W. D.; Lewis, T.; Fletcher, R. J.; Guss, J. M.; Silman, I.; Sussman, J. L. Protein Sci 2000, 9, 1063–1072.
14. Greenblatt, H. M.; Silman, I.; Sussman, J. L. Drug Develop Res 2000, 50, 573–583.
15. Silman, I.; Sussman, J. L. Cholinesterases and Cholinesterase Inhibitors; Giacobini, E., Ed.; Martin Dunitz: London, 2000; pp 9–25.
16. Millard, C. B.; Koellner, G.; Ordentlich, A.; Shafferman, A.; Silman, I.; Sussman, J. L. J Am Chem Soc 1999, 121, 9883–9884.
17. Bar-On, P.; Millard, C. B.; Harel, M.; Dvir, H.; Enz, A.; Sussman, J. L.; Silman, I. Biochemistry 2002, 41, 3555–3564.
18. Dvir, H.; Wong, D. M.; Harel, M.; Barril, X.; Orozco, M.; Luque, F. J.; Munoz-Torrero, D.; Camps, P.; Rosenberry, T. L.; Silman, I.; Sussman, J. L. Biochemistry 2002, 41, 2970–2981.
19. Wolberg, G. Digital Image Warping; Wiley-IEEE Press, New York, 1990.
20. Krebs, W. G.; Gerstein, M. Nucleic Acids Res 2000, 28, 1665–1675.
21. Kleywegt, G. J. Acta Cryst 1996, D52, 842–857.
22. Kleywegt, G. J. Uppsala Software Factory—LSQMAN Manual; Uppsala Software Factory, 2002; http://xray.bmc.uu.se/~gerard/manuals/lsqman_man.html#S71.
23. Jones, T. A.; Zou, J.-Y.; Cowan, S. W.; Kjeldgaard, M. Acta Cryst 1991, A47, 110–119.
24. Sayle, R. A.; Milner-White, E. J. TIBS 1995, 20, 374–376.
25. Mediaconvert; SGI, 2002; http://www.sgi.com.

26. QuickTime; Apple Computer, 2002; http://www.apple.com/quicktime/.
27. Quinn, D. M. Chem Rev 1987, 87, 955–975.
28. Aldridge, W. N.; Reiner, E. Enzyme Inhibitors as Substrates: Interactions of Esterases with Esters of Organophosphorus and Carbamic Acids; North-Holland Publishing: Amsterdam, 1972; Vol 26.
29. Koelle, G. B. Cholinesterases and Anticholinesterase Agents; Springer-Verlag: Heidelberg, 1963; Vol 15.
30. Millard, C. B.; Kryger, G.; Ordentlich, A.; Harel, M.; Raves, M.; Greenblatt, H. M.; Segall, Y.; Barak, D.; Shafferman, A.; Silman, I.; Sussman, J. L. Biochemistry 1999, 38, 7032–7039.
31. Giles, K.; Raves, M. L.; Silman, I.; Sussman, J. L. Theoretical and Computational Methods in Genome Research; Suhai, S., Ed.; Plenum Press: New York, 1997; pp 303–315.
32. Karlsson, E.; Harvey, A. L.; Cerveñansky, C.; Kleywegt, G. J.; Harel, M.; Silman, I.; Sussman, J. L. Enzymes from Snake Venoms; Bailey, G. S., Ed.; Alaken: Fort Collins, CO, 1998; pp 633–688.
33. Harel, M.; Kleywegt, G. J.; Ravelli, R. B. G.; Silman, I.; Sussman, J. L. Structure 1995, 3, 1355–1366.
34. Radic, Z.; Quinn, D. M.; Vellom, D. C.; Camp, S.; Taylor, P. J Biol Chem 1995, 270, 20391–20399.
35. Marchot, P.; Bourne, Y.; Prowse, C. N.; Bougis, P. E.; Taylor, P. Toxicon 1998, 36, 1613–1622.
36. De Ferrari, G. V.; Mallender, W. D.; Inestrosa, N. C.; Rosenberry, T. L. J Biol Chem 2001, 276, 23282–23287.
37. Eastman, J.; Wilson, E. J.; Cerveñansky, C.; Rosenberry, T. L. J Biol Chem 1995, 270, 19694–19701.
38. Szegletes, T.; Mallender, W. D.; Thomas, P. J.; Rosenberry, T. L. Biochemistry 1999, 38, 122–133.
39. Mallender, W. D.; Szegletes, T.; Rosenberry, T. L. Biochemistry 2000, 39, 7753–7763.
40. Shi, J.; Boyd, A. E.; Radic, Z.; Taylor, P. J Biol Chem 2001, 276, 42196–42204.
41. Tai, K.; Shen, T.; Henchman, R. H.; Bourne, Y.; Marchot, P.; McCammon, J. A. J Am Chem Soc 2002, 124, 6153–6161.
42. Jacobs, D. J.; Rader, A. J.; Kuhn, L. A.; Thorpe, M. F. Proteins 2001, 44, 150–165.
43. Ming, D.; Kong, Y.; Lambert, M. A.; Huang, Z.; Ma, J. Proc Natl Acad Sci USA 2002, 99, 8620–8625.
44. Godzik, A. Protein Sci 1996, 5, 1325–1338.
45. Vonrhein, C.; Schlauderer, G. J.; Schulz, G. E. Structure 1995, 3, 483–490.
46. Felder, C. E.; Botti, S. A.; Lifson, S.; Silman, I.; Sussman, J. L. J Mol Graphics Model 1997, 15, 318–327.